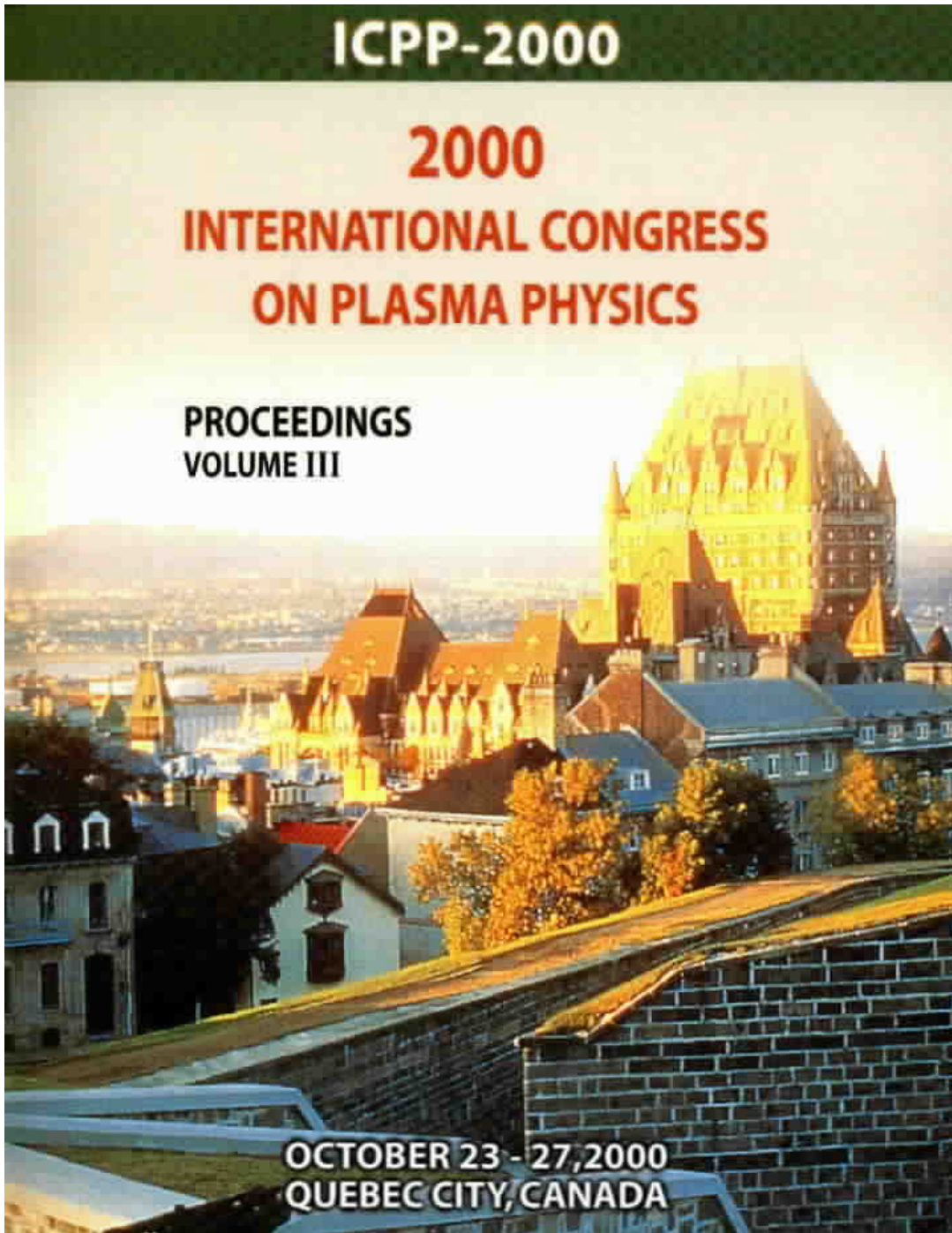


ICPP-2000

2000
INTERNATIONAL CONGRESS
ON PLASMA PHYSICS

PROCEEDINGS
VOLUME III

OCTOBER 23 - 27, 2000
QUEBEC CITY, CANADA



Investigation of Electromagnetic Field Penetration in ICP and Weakly-Magnetized ICP Discharges

John D. Evans*, Francis F. Chen** and Donald Amush***
University of California, Los Angeles, California, USA

The relationship between the penetration of RF fields and power deposition in ICP discharges is not fully understood. In particular, it is important to determine how non-local power deposition affects the plasma properties of low pressure ICP discharges. To this end, investigation of RF field penetration is performed using a multi-turn loop antenna wrapped around a cylindrical squat bell jar (Fig. 1), rather than the more complicated “stove-top” antenna configuration. An RF-compensated Langmuir probe and a B_z -dot probe (oriented to measure B_z , the vertical z component of \mathbf{B}_{RF}) are used to measure $N(r)$, $T_e(r)$ and $B_z(r)$ in the plane of the antenna. Simplicity of antenna geometry facilitates the comparison between measured RF penetration depths (L_{sd}) and classical collisional theory using the HELIC [1] code. $N(r)$ and $T_e(r)$ are used as inputs to HELIC to calculate \mathbf{s} , the plasma conductivity. Plasma currents are calculated using Ohm’s law, $\mathbf{J} = \mathbf{s} \bullet \mathbf{E}$, which assumes a local relationship between \mathbf{J} and \mathbf{E} through $\mathbf{s}(r)$, and are used together with the antenna currents to compute theoretical $B_z(r)$. Good agreement is obtained between measured $B_z(r)$ and HELIC curves in collisional plasmas for which Ohm’s law is valid. Discrepancies between measurements and HELIC profiles indicate possible deviations from collisional behavior, most likely due to the inapplicability of Ohm’s law in regimes where non-local behavior [2] dominates.

A wide range of plasma parameters is studied, examining 3 collisional regimes [2]: “normal” (classic collisional, $\omega < \nu_{en}$, $L_{sd} < \lambda_{mfp}$), “high frequency” ($\omega > \nu_{en}$), and “anomalous” (non-local, $L_{sd} > \lambda_{mfp}$). Here, ν_{en} is the electron-neutral collision frequency ($\cong \nu_{coll}$) and λ_{mfp} is the electron mean free path. Effects of an applied static \mathbf{B}_o -field on RF field penetration are also investigated. In nearly all cases, the observed profiles are well understood. Excellent agreement is obtained between collisional theory and experiment in weakly magnetized and “normal” collisional regimes. Deviations of measured L_{sd} ’s from collisional theory are observed at high frequency ($\omega > \nu_{en}$) and low pressure P_o ($L_{sd} > \lambda_{mfp}$), as expected. Interference and “standing-wave-like” phenomena are observed at high P_{RF} while operating in or near the “anomalous” regime. However, the dependence of this observed behavior on P_o (ν_{en}) is in apparent contradiction to the predictions of the theory of the anomalous skin effect [2] (ASE), which is the electromagnetic analog of the well known electrostatic Debye shielding effect.

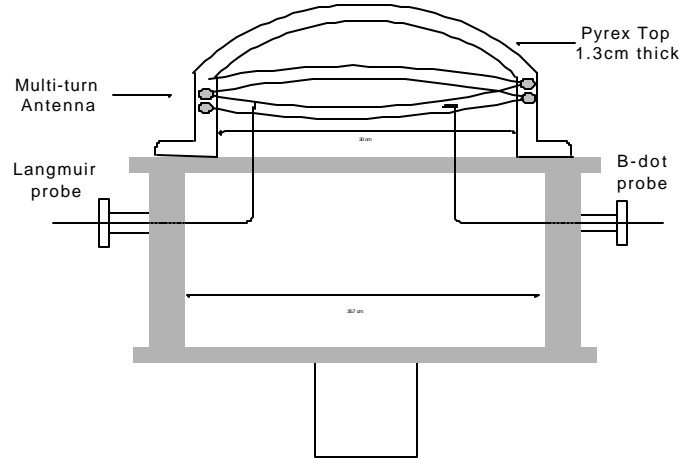


Fig. 1. Schematic diagram of the experimental setup, including antenna, dogleg Langmuir and B-dot probes. Probe heights and antenna locations are arranged so that profiles are obtained in the plane of the antenna. Typical operating parameters are: $N_p \sim 5 \cdot 10^{10} - 5 \cdot 10^{11} \text{ cm}^{-3}$, $P_{RF} \approx 400\text{W}$, $T_e \sim 2-4\text{eV}$, $P_0 = 1-20\text{mT}$, $f_{RF} \sim 2-7\text{MHz}$.

Fig. 2 (left) shows a semi-log plot of $B_z(r)$ obtained in a collisional plasma. Least squares fits to the “left” and “right” branches yield $L_{sd} = 3.4\text{cm}$ and 2.8cm , respectively. Comparison (right) between collisional theory (L_{coll} , red) and experiment (L_{sd} , dashes) agree to within $\pm 10\%$. Collisionless skin depth ($L_{less} \equiv c/\omega_{pe}$) is also shown for comparison (purple).

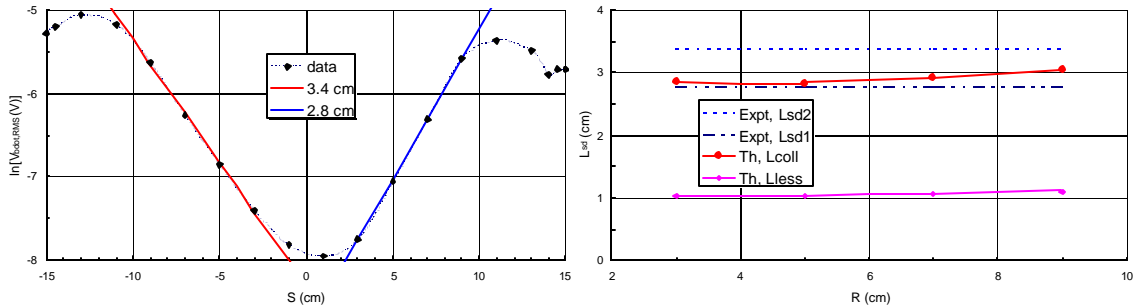


Fig. 2. Semi-log plots of B-dot profile (left) in “normal” collisional regime (300W, 2MHz, 20mT). Edge features (“wings”) are probably due to the effects of induced currents in nearby conductors. Least squares fits yield experimental L_{sd} ’s (right, dashes), in good agreement with collisional theory (L_{coll} , red).

A similar comparison vs. P_0 (1-20mT) is made in “high frequency” discharges. Reasonable agreement (Fig. 3) is seen at higher P_0 ; data diverges from collisional theory [2] at lower P_0 .

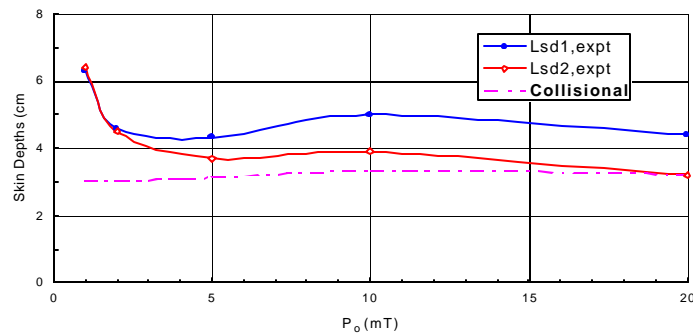


Fig. 3. Comparison between experimental L_{sd} ’s and collisional theory (pink). 200W, 6.78MHz, $P_0 = 1-20\text{mT}$.

At $f_{RF}=2\text{MHz}$, $P_o=5\text{-}20\text{mT}$, and $P_{RF}\sim 400\text{W}$, local minima (“nodes”) and rapid phase discontinuities (“jumps”) of 180° in $B_z(r)$ are observed (Fig. 4), indicating interference and/or standing-wave-like behavior, most apparent at highest P_o . Since f_{RF} is too high to excite ion-acoustic instabilities and too low for electron plasma waves, and $\mathbf{B}_o=0$, then these effects are not accounted for in linear plasma theory. Such effects have been observed by others [3], and

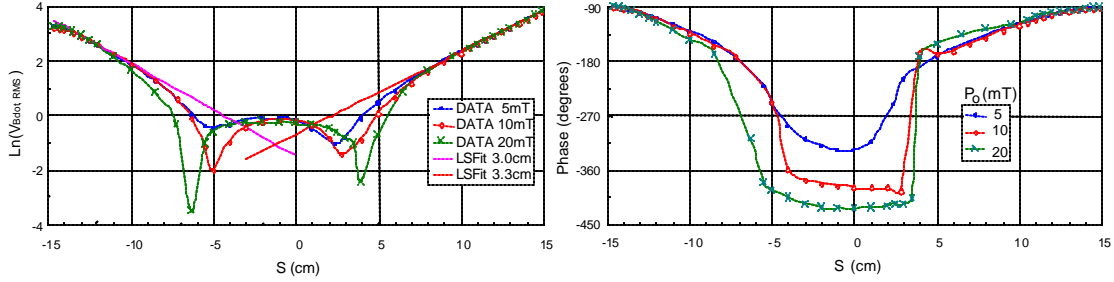


Fig. 4. $\text{Ln}(B_z)$ amplitude (left) and phase (right) radial profiles, for $P_o = 5\text{-}20\text{ mT}$, 400W , 2MHz . Local minima (nodes) and $\sim 180^\circ$ phase “jumps” at $|s|\sim 5\text{cm}$ are indications of interference and/or standing-wave-like behavior. These effects become more apparent as P_o (n_{en}) increases, in apparent contradiction to ASE theory.

interpreted as manifestations of ASE [2-4]. Careful examination of the $B_z(r)$ data and HELIC curves (Fig. 5) for $P_o=5\text{mT}$ (left) and 20mT (right) shows that the field behavior in the outer region ($|R|>a/2$) indeed converges to the HELIC collisional result as P_o increases, consistent with ASE theory. However, the depth of the nodes and the steepness of the phase jumps increase with P_o . These phenomena become more apparent as collisionality increases and ASE supposedly weakens, indicating they are probably not manifestations of ASE. Since nodes in $B_z(r)$ can be produced in ICP’s only by internal currents flowing out of phase with the antenna B_z -field, yet another mechanism of non-local ($\mathbf{J} \neq \sigma \bullet \mathbf{E}$) behavior is operative.

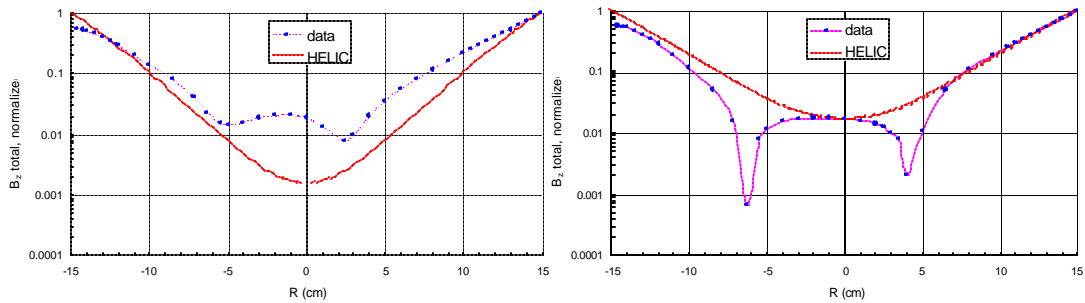


Fig. 5. Comparison between measured B_z -dot profiles and HELIC code at $P_o=5\text{mT}$ (left) and 20 mT (right), illustrating the expected transition of RF-field behavior for $R>a/2$ from anomalous to collisional as P_o increases, consistent with ASE theory. However, the local minima (“nodes”) are more pronounced at higher P_o , indicating that ASE is not the cause of the interference phenomena. Non-local behavior ($\mathbf{J} \neq \sigma \bullet \mathbf{E}$) is evident.

At lower $P_{RF}=200\text{W}$ and $P_o=5\text{mT}$, ASE theory predicts strongly anomalous field penetration, which is readily observed (Fig. 6, left) by comparing the measured profile (blue)

to the HELIC (red) curve. Application of a small \mathbf{B}_o -field, using a large magnet coil just below the antenna, apparently suppresses the ASE. This effect can be seen at $\mathbf{B}_o \sim 5\text{G}$, and is evidenced by improved agreement between the data and the HELIC curve for $\mathbf{B}_o=20\text{G}$ (right).

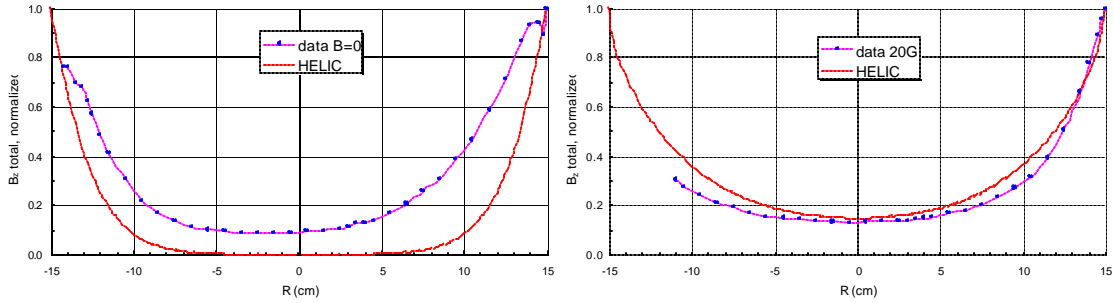


Fig. 6. Comparison of RF field penetration in an unmagnetized (left) and weakly-magnetized (right, $B_o=20\text{G}$) ICP, otherwise operating in the anomalous regime (2MHz , 5mT). Anomalous field penetration appears to be suppressed by application of a static \mathbf{B}_o -field, as shown by agreement between the 20G data and HELIC curves.

A summary of these results is shown below (Fig. 7), where the collisional regimes for each experiment are indicated as points on this plot of non-locality versus normalized frequency, following Fig. 1 of [2]. Deviation from classical collisional behavior is indicated qualitatively by relative size of data markers (e.g. increase in depth of nodes and phase jumps {dark squares} as the regime $\{P_o\}$ changes from “anomalous” to “normal” is indicated thus).

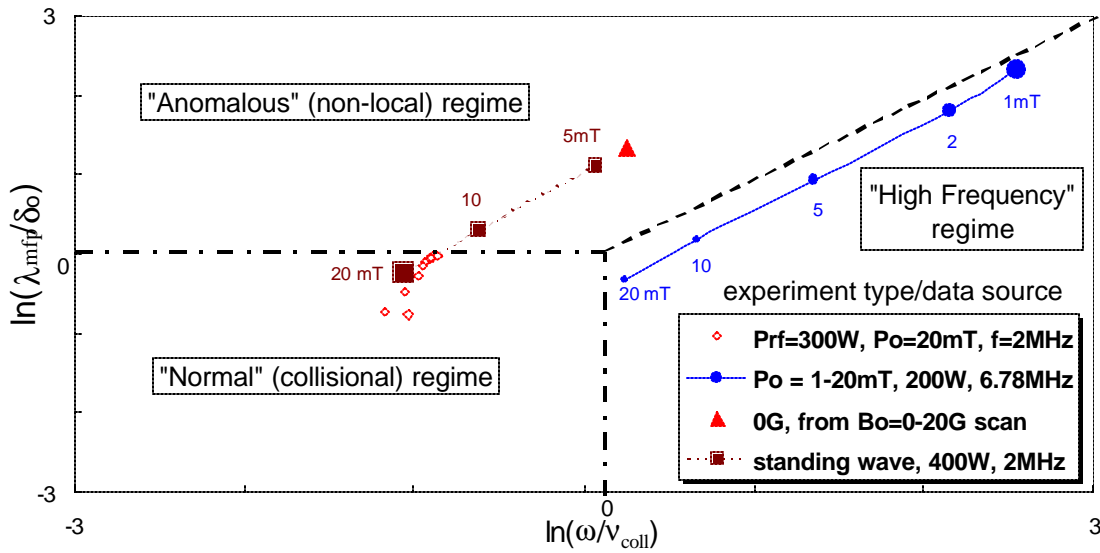


Fig. 7. Collisional regimes in parameter space for each experiment: ASE non-locality parameter $\ln(\lambda_{mfp}/d_o)$ vs $\ln(\omega/v_{coll})$, where $d_o \propto (c/w_{pe}) \cdot (1 + n_{coll}^2/w^2)^{1/4}$ and $n_{coll} \propto$ electron collisional frequency ($\equiv n_{en}$ in these discharges).

* jdevans@ea.ucla.edu ** ffchen@ee.ucla.edu *** darnush@ucla.edu

- [1] Arnush, D. and Chen, F.F., *Phys. Plasmas* **5**, (1998), 1239.
- [2] Kolobov, V.I. and Economou, D.J., *PSST* **6**, (1997), R1-17, and references therein.
- [3] Joye, B. and Schneider, H., *Helv. Phys. Acta* **51** (1978), 804.
- [4] Sayasov, Y. S., *Helv. Phys. Acta* **52** (1979), 288.